



Published in final edited form as:

Anal Chem. 2008 April 15; 80(8): 2881–2887. doi:10.1021/ac070038v.

Monoclonal Behavior of Molecularly Imprinted Polymer Nanoparticles in Capillary Electrochromatography

Feliciano Priego-Capote^{†,‡}, Lei Ye[‡], Sadia Shakil[‡], Shahab A. Shamsi[§], and Staffan Nilsson^{*,‡}

[†]Department of Analytical Chemistry, Córdoba University, Annex C-3 Building, Campus of Rabanales, E-14071 Córdoba, Spain

[‡]Department of Pure and Applied Biochemistry, Center for Chemistry and Chemical Engineering, Lund University, P.O. Box 124, SE-221 00 Lund, Sweden

[§]Department of Chemistry, Center of Biotechnology and Drug Design, Georgia State University, Atlanta, Georgia 30303

Abstract

A new approach based on miniemulsion polymerization is demonstrated for synthesis of molecularly imprinted nanoparticles (MIP-NP; 30–150 nm) with “monoclonal” binding behavior. The performance of the MIP nanoparticles is characterized with partial filling capillary electrochromatography, for the analysis of *rac*-propranolol, where (*S*)-propranolol is used as a template. In contrast to previous HPLC and CEC methods based on the use of MIPs, there is no apparent tailing for the enantiomer peaks, and baseline separation with 25 000–60 000 plate number is achieved. These effects are attributed to reduction of the MIP site heterogeneity by means of peripheral location of the core cross-linked NP and to MIP-binding sites with the same ordered radial orientation. This new MIP approach is based on the substitution of the functional monomers with a surfactant monomer, sodium *N*-undecenoyl glycinate (SUG) for improved inclusion in the MIP-NP structure and to the use of a miniemulsion in the MIP-NP synthesis. The feasibility of working primarily with aqueous electrolytes (10 mM phosphate with a 20% acetonitrile at pH 7) is attributable to the micellar character of the MIP-NPs, provided by the inclusion of the SUG monomers in the structure. To our knowledge this is the first example of “monoclonal” MIP-NPs incorporated in CEC separations of drug enantiomers.

Capillary electrochromatography (CEC) has been extensively studied during the last 15 years and has proved to be a versatile technique for analytical separations and studies of molecular interactions.^{1–3} CEC combines the high efficiency of CE with the selectivity and diverse stationary phases of HPLC.^{4,5} Molecularly imprinted polymers (MIPs), which are cross-linked polymer materials with tailor-made recognition properties for specific analyte templates,⁶ have been suggested as suitable stationary and pseudostationary phases (PSPs) in CEC when a predetermined selectivity is required.^{7–10} Nanoparticles in PSP-CEC have been used for highly efficient separation (700 000 plates/m) of small, neutral compounds.¹¹

The partial filling^{12,13} format possesses several benefits compared to traditional CEC modes based on monolithic¹⁴ or packed columns.¹⁵ First, a fresh and new MIP nanoparticle (NP) phase is used for each analysis, which eliminates carryover when samples with complex matrixes are analyzed. Second, the length and type of the particle phase can easily be tailored

for each separation without changing the separation capillary or column.¹⁶ Third, time-consuming and tedious packing is not required and adverse effects of retaining frits are circumvented.¹⁷

A long-standing challenge for MIP-based adsorbents is to avoid or reduce the presence of heterogeneous binding sites with a range of affinity for the target molecule that is correlated to the concentration of analyzed template.¹⁸ When MIPs are used as a stationary phase for chiral separation in HPLC or CEC, they often yield inadequate resolution and, without exception, a peak-tailing corresponding to the specific template enantiomer. This template tailing is due to the wide distribution of sites with varying association and dissociation kinetics. For many analytical applications, a new generation of MIPs with homogeneous binding sites (monoclonal MIPs) is highly desirable, but requires new strategies for MIP preparation. Toward this end, we have studied the synthesis of MIP-NPs limited to a single binding site population on the particle surface, as suggested in Figure 1. For MIP-NP CEC separations, relatively weak interactions are of interest between template and surface-exposed binding sites, which thus would allow fast chiral separation.¹⁹

Conventional approaches for the preparation of spherical MIP nanoparticles are based on precipitation²⁰ and emulsion polymerization techniques.²¹ The polymerization processes in these systems are under kinetic control, resulting in nonideal MIP beads that have inhomogeneous binding sites and restricted particle size.

The objective of this work was to take advantage of a potential thermodynamic control for design of nanoparticles. With this technique, small “nanoreactors” are developed for the formation of nanoparticles, with the monomers and the template molecule incorporated at the beginning of the polymerization. Thermodynamic control can be achieved by suspension polymerization, although this can result in imprinted particles that are rather large and nonuniform. In addition, the particles exhibit relatively low interfacial surface area, thus restricting template binding.²² An alternative proposed by Ugelstad et al. is to scale down the droplet size of the suspension to nanometers by suppressing the diffusion process in the continuous phase, thereby creating a stable emulsion, of homogeneous size, called a miniemulsion.²³ In miniemulsion polymerization, no organic solvents are used, the reaction is easy to control thermally, and high polymerization rates can be achieved due to radical compartmentalization. An additional advantage is that water-insoluble reagents can be used. The components for obtaining MIP nanoparticles by miniemulsion polymerization consist of the template molecule, a functional monomer, a cross-linker, an initiator, a small amount of nonpolar solvent, water, and a surfactant in order to generate the miniemulsion.²⁴ Droplet nucleation is the main basis of miniemulsion polymerization, which enables the use of hydrophobic reactants as the need for mass transfer through the aqueous phase is minimized. Thus, separation materials can be obtained as very small imprinted particles.²⁵

Shamsi et al. have demonstrated the utility and advantages of polymeric surfactants as pseudostationary phases for micellar electrokinetic chromatography (MEKC), using high proportions of organic solvents without changes in micellar properties.^{26,27} Structurally, polymeric surfactants are very similar to conventional micelles, but form spherical aggregates, which are covalently linked via the hydrophobic tails, while the polar head groups remain on the outside of the aggregate.^{28,29} Several studies have shown the influence on chemical selectivity in MEKC^{30–32} is dependent on the polar head group and the hydrocarbon chain length. Therefore, it would be favorable to incorporate such polymeric surfactant monomers in the MIP-NP process.

EXPERIMENTAL SECTION

Reagents and Chemicals

Ethylene glycol dimethacrylate (EDMA) and hexadecane were purchased from Aldrich (Gillingham, UK) and used without further purification. The (*R*)- and (*S*)-propranolol, as hydrochloride monohydrates, were a kind gift from AstraZeneca R&D Mölndal (Mölndal, Sweden). The (*S*)-propranolol was converted to its free base form by dissolving the hydrochloride form in an aqueous saturated sodium carbonate solution and by subsequent extraction three times in chloroform. The organic phase was dried over anhydrous sodium sulfate, filtered, and evaporated. It was stored at $-20\text{ }^{\circ}\text{C}$ until use. The *rac*-propranolol hydrochloride was obtained from Fluka (Buchs, Switzerland). The 2,2'-azobis(isobutyronitrile) (AIBN) was obtained from Sigma (St. Louis, MO) and recrystallized from methanol before use. Water was purified by a MilliQ purification system (Millipore, Bedford, MA), (*S*)-[4- ^3H]-Propranolol (specific activity 555 GBq mmol^{-1} , $66.7\text{ }\mu\text{M}$ solution in ethanol) was purchased from NEN Life Science Products, Inc. (Boston, MA). Scintillation liquid, Ecoscint A, was from National Diagnostics (Atlanta, GA), and all other chemicals were from Merck (Hohenbrunn, Germany) and were used as received. Sodium *N*-undecenoyl glycinate (SUG) was synthesized according to a procedure previously described³³ and used as surfactant monomer for the synthesis of nanoparticles.

Preparation, Sorting, and Purification of Nanoparticles

Nonimprinted polymer nanoparticles (NIP-NP) were prepared by mixing 182 mg (0.69 mmol) of surfactant monomer (SUG), 0.6 g of EDMA (3 mmol), 25 mg (0.11 mmol) of hexadecane, and 13 mg (0.08 mmol) of AIBN with 5 mL of water in a glass test tube. When the MIP-NPs were prepared, 16 mg (0.0625 mmol) of (*S*)-propranolol was added to the monomer phase. The two phases were dispersed by sonication in an ultrasonic bath for 2 min at room temperature followed by sonication for 2 min (4 periods of 30 s in order to avoid the excessive heating of the mixture) with an ultrasonic probe (Heat Systems-Ultrasonics, Inc., model W-380, 20 kHz, 50% power 475 W), which was directly immersed into the test tube. The aim of the second sonication step was to form the miniemulsion prior to the polymerization. The polymerization was carried out at $70\text{ }^{\circ}\text{C}$ for 16 h.

The sorting step (Figure 2) was performed by filtration with 1- μm -pore size membranes using a centrifugal microsystem (Amicon Division, Danvers, MA) for 10 min, after which the solid phase was resuspended in acetic acid/acetonitrile (1:3 v/v), sonicated for 10 min in an ultrasonic bath, agitated for 30 min, and was repeated two times, but in the last one, only acetonitrile (ACN) was used for suspension of the particles. The objective of this washing procedure was to ensure the removal of the template from the imprinted nanoparticles. The polymer nanoparticles were stored at $5\text{ }^{\circ}\text{C}$ until further use. **Caution:** The chemicals used for polymer synthesis are toxic. All the reagents should be handled in a ventilated fume hood. Sample treatment with the ultrasonic probe should be carried out in an isolated sound-proof cabinet.

Characterization of Nanoparticles

Particle morphology was evaluated using SEM measurements carried out on a JSM-6700F field emission scanning electron microscope (JEOL, Tokyo, Japan). The size distribution of the MIP-NPs was determined by dynamic light scattering with a Zetasizer Nano ZS (Malvern Instruments, Worcestershire, UK). Prior to size determination, the polymer samples were diluted 10 times with water containing 10% (v/v) ethanol.

Radioligand Binding Analysis

The MIP and NIP nanoparticles were suspended in citrate buffer (25 mM, pH 6.0) containing 50% (v/v) ACN at a final concentration of 1.0 mg/mL. The radioligand (*S*)-propranolol was added to give a final concentration of 6 nM. The samples were incubated at ambient temperature for 16 h to ensure equilibrium binding. After the incubation, the samples were centrifuged, and the supernatant (500 μ L) was withdrawn and mixed with 10 mL of Ecoscint A for radioactivity measurement by liquid scintillation counting. A model 1219 Rackbeta β -radiation counter from LKB Wallac (Sollentuna, Sweden) was used. The amount of labeled (*S*)-propranolol bound to polymer nanoparticles was calculated by subtraction of the free fraction from the total amount added.

Capillary Electrochromatography

All CEC experiments were performed on a Beckman P/ACE System 5010 (Beckman, Fullerton, CA) equipped with a UV detector. Fused-silica capillaries (75- μ m i.d., 375- μ m o.d.) with 37-cm total length and 29.4-cm effective length were obtained from Polymicro Technologies (Phoenix, AZ). The electrolyte consisted of 10 mM phosphate buffer containing 20% acetonitrile solution at pH 7, which was daily made from a stock solution and degassed by sonication. Prior to CEC analysis, the capillary was rinsed every day with 1 M NaOH, water, and electrolyte. The capillary was also rinsed with 1 M NaOH and electrolyte between consecutive runs in order to remove nanoparticles adsorbed to the capillary wall and make the analyses more reproducible. NIP or MIP nanoparticles suspended in the electrolyte at a concentration of 10 mg/mL were injected hydrodynamically at 0.5 psi for 5–25 s. Samples, (*R*)-propranolol, (*S*)-propranolol, and *rac*-propranolol, prepared from a 20 mM stock solution in buffer and diluted to proper concentrations in water, were injected electrokinetically for 3 s at 6 kV. The separation voltage was varied between 10 and 30 kV, and the temperature of the capillary varied between 20 and 50 $^{\circ}$ C. UV detection was performed at 214 nm.

The plate number was calculated from the equation $N = 5.54 (t_R/W_{1/2})^2$, where t_R is the retention time for the peak and $W_{1/2}$ is the peak width at half-height of the peak signal. The peak tailing was evaluated by the asymmetry factor calculated from the ratio a/b , a being the distance from the elution time (at the maximum of the peak) to the time at which the peak ends and b being the distance from the time at which the peak starts to the elution time.

RESULTS AND DISCUSSION

Characterization of Nanoparticles

The preliminary studies indicated that the ratio between the template and the functionalized surfactant monomer should be fixed at 1:11 while the ratio between surfactant monomer and cross-linker was optimized to 1:4.4. The use of higher or lower cross-linker ratio resulted in unstable emulsions, which gave large particles with fast sedimentation behavior not suitable for PSP-CEC. The fact that the MIP-NP had good suspension stability in the water-rich electrolyte indicates that a high charge density exists on the surface of the nanoparticles, which can be achieved only by the surfactant molecules that are covalently fixed in the nanoparticles. The template-monomer interactions are governed by an equilibrium process; thus, a large amount of monomer is required in order to displace the equilibrium to form the template-monomer complex. However, excess of free monomers leads to the formation of nonspecific binding sites and heterogeneous binding positions.³⁴

As the new approach used for MIP-NP synthesis omitted the commonly used functional monomer/s, preliminary studies were performed to characterize the particles obtained, by SEM measurements in order to determine particle size and morphology. The SEM images shown in Figure 3 reveal spherical NIP and MIP particles with size ranges from 30 to 80 nm and from

80 to 120 nm, respectively. The presence of the template molecule during the nanoparticle polymerization had slight influence on the particle size, as has been observed in other reaction systems for preparing molecularly imprinted nanoparticles.⁸ Indicated ranges are approximate as no exact data about polydispersity can be obtained from SEM measurements alone. However, the presence of some aggregates was detected for the MIP-NPs as these SEM measurements were performed before sorting and purification (see Figure 2).

The particle size distribution was further studied by dynamic light scattering measurement. In the case of the NIP nanoparticles, two Gaussian peaks were obtained at 68 (range from 35 to 105 nm) and 313 nm (from 200 to 1000 nm) with a proportion of 63.93 and 28.26%, respectively. For the MIP nanoparticles, two Gaussian peaks were obtained at 80 (range from 30 to 150 nm) and 291.9 nm (from 200 to 1000 nm) with a proportion of 71.22 and 20.46%, respectively.

Imprinted particles were sorted and purified as outlined in Figure 2 to remove particles with larger size, which were ascribed to the formation of aggregates. Thus, nanoparticles with more narrow size distribution were obtained, to achieve a more condensed NP plug for the CEC analysis. CE analyses of purified MIP-NPs were performed to evaluate the retention behavior of the MIP-NP in the capillary. Figure 4 illustrates the electropherogram of nanoparticles at 10 mg/mL after sorting and purification (Figure 2.). Particles were injected hydrodynamically for 5 s, and the migration of the particles remained as a plug without significant separation between particles of different mass-to-charge ratio. Removal of the template molecule in the sorting and purification process (Figure 2) was efficient as well, as no peak was obtained at the elution window of (*S*)-propranolol (1.4–1.7 min).

Radioligand Binding Assays

A batch mode equilibrium binding experiment was carried out to confirm that the present surface imprinting contributed to increased template binding of imprinted as compared to nonimprinted nanoparticles. After polymer samples were incubated, the radioligand uptake by the imprinted nanoparticles (7.6%) was three times higher than the nonimprinted nanoparticles (2.4%), showing an obvious imprinting effect. The overall template uptake by the present imprinted nanoparticles was much lower than that of propranolol-imprinted microspheres made by precipitation polymerization, which bound more than 70% of the radioligand under the same condition.³⁵ However, the optional separation range can be enhanced by using a longer nanoparticle plug or the continuous full-filling approach.¹¹

The reduced apparent template affinity in the present system may partly be explained by the present MIP preparation methodology, which generates only surface binding sites on the nanoparticle, whereas the precipitation polymerization used previously produces a distribution of imprinted sites throughout the polymer matrix. The reduced affinity may also be attributed to the use of the different solvents in these experiments. However, this lower affinity can be utilized by a highly efficient CEC separation approach.¹¹

MIP-NP CEC

The MIP nanoparticles were tested as PSP in CEC.^{12,13} A partial filling format was utilized, by which a plug of nanoparticles suspended in electrolyte is injected prior to the sample. Provided there is a proper mobility difference between the analytes and the nanoparticles, the analytes will start to migrate through the nanoparticle plug as a voltage is applied over the capillary. During their passage through the capillary, the analytes will interact with and become separated on the MIP nanoparticles in the plug.

It is well-known that the solvent employed for the MIP-NP synthesis plays a key role in the recognition process by governing the strength of noncovalent interactions in addition to its influence on the polymer morphology.^{36,37} The best imprinting porogens, for accentuating the binding strengths, are solvents with very low dielectric constants, such as toluene and dichloromethane. This is also valid for the solvent used where the imprinting effect is demonstrated, as is the case of the electrolyte in CEC. Generally, the more polar the electrolyte, the weaker the resulting recognition effect becomes as a consequence of the influence of the solvent polarity on noncovalent interactions.

The use of more polar solvents will inevitably weaken the interaction forces between the template and the functional monomers, resulting in lower affinity recognition. Inclusion of functionalized surfactant monomer in the nanoparticles structure imparts amphiphilic character to the synthesized nanoparticles, enabling the use of more aqueous electrolyte. This is advantageous, as the majority of published MIP-CEC separations are limited to a low pH electrolyte and a high percentage of organic modifier.^{8,9,11} The use of more aqueous electrolytes decreases the interactions between template and imprinted nanoparticles, improves separation kinetics, maintains higher theoretical plate numbers achievable in CEC, and provides suitable MIP retention of analyte.

For this work, the composition of the MIP-CEC electrolyte in terms of concentration of phosphate and percentage of acetonitrile as modifier was optimized. The running buffer is composed of a low phosphate concentration (10 mM) at pH 7.0 in order to reduce the separation current and avoid Joule heating. The difference of mobility between sample and nanoparticles plug was increased as compared with earlier used electrolytes. Values between 0 and 90% ACN (v/v) were tested. The optimal proportion of aqueous buffer/ACN was found to be 80/20% (v/v) for maintaining the nanoparticles suspension with minimal sedimentation. In addition, this ACN concentration allows higher reproducibility of the particle injections without extensive longitudinal broadening of the nanoparticle plug during MIP-NP-CEC analysis.

The amount of MIP-NPs (5–10 µg/analysis) for each CEC analysis was optimized by modification of the injection time from 5 to 25 s. Separation of the propranolol enantiomers was obtained for all tested injection times, but the optimal particle injection time was 10 s. As shown in Figure 5, shorter plug injection time such as 5 s provided poor enantioseparations due to the short contact time between the sample and the nanoparticle plug. On the other hand, efficient separations were obtained for the longer injection time of 25 s, but the peak height was considerably lower due to adsorption and more pronounced associations in the MIP plug. The capillary temperature had a significant influence on the peak shapes due to modified enantiomer nanoparticle interactions. Thus, the interaction that provides the most efficient separations in terms of resolution and peak tailing was obtained at 30 °C.

Figure 6 illustrates the separation of *rac*-propranolol by CEC depicting the characteristic elution order and the selective retention of the imprinted molecule (A) as compared to the same analysis but injecting only (*S*)-propranolol (B). Thus, imprinting the nanoparticles against (*S*)-propranolol, as in this study, provides a selector that can be used to separate racemic propranolol based on the selection and subsequently the increased retention of the template enantiomer. The peak tailing was evaluated by the asymmetry factor for both peaks, which were 1.17 and 1.15 for (*R*)- and (*S*)-propranolol (template), respectively. As the asymmetry factor is similar for both enantiomers, the tailing of both peaks can be attributed to the electrochromatographic conditions.

Note that in contrast to previous MIP-based HPLC or CEC separations, the peak corresponding to the template molecule does not present any tailing as a consequence of uniform interactions between template molecule and imprinting site. This is attributed to weak and homogeneous

interactions between template and imprinting sites, which separate the two enantiomers without any significant deformation of the peaks, particularly that corresponding to (*S*)-propranolol. The plate number achieved was in the range of 25 000–60 000 plates/m.

For unambiguous identification of the CEC peaks, additional tests were made to confirm the MIP-NP enantioselectivity by overloading the *rac*-propranolol sample with either (*R*)- or (*S*)-propranolol. A corresponding increase in peak height was achieved in the electropherogram when sample was spiked with (*S*)- or (*R*)-propranolol, respectively (Figure 7A and B), providing additional evidence that successful imprinting was achieved with the new described MIP-NP methodology.

CONCLUSIONS

For the first time to our knowledge, “monoclonal” MIPs has been synthesized and demonstrated, here in chromatography-based separation of a racemic mixture giving nontailing peaks. Baseline separations with plate number between 25 000 and 60 000 have been obtained for enantiomeric separations of *rac*-propranolol by CEC using MIP nanoparticles toward (*S*)-propranolol as pseudostationary phase. The backgrounds for these excellent results are the following. First, the binding sites located close to the peripheral part of the core cross-linked nanoparticles are expected to have the same ordered radial orientation, because the new synthetic strategy based on miniemulsion polymerization using a surfactant monomer SUG provided homogeneous sites. Second, the small size (30–150 nm) of the imprinted nanoparticles results in reduced number of recognition sites for each nanoparticle. Finally, the weak interactions between the MIP nanoparticles and enantiomers enable efficient separation of both enantiomers. These weak interactions can partly be explained by operating with more aqueous electrolytes (containing a low proportion of acetonitrile (20%)).

The achievable size of nanoparticles points to the possibility of producing single-imprint MIP-NPs. This could open up future strategies toward single-molecule extraction³⁹ and detection.^{40–43} The inclusion of the surfactant monomer into the nanoparticles' structure enabled us to operate in CEC with more aqueous electrolytes, which was attributed to the new structure of the nanoparticles with a hydrophobic core region and a hydrophilic surface. This new approach opens new perspectives for further research on the preparation of highly selective MIPs in aqueous media and also for LC and CEC applications, or for sampling of analytes or specific removal of toxic reagents.

ACKNOWLEDGMENT

F.P.-C. is grateful to the Ministerio de Educación, Cultura y Deportes for an FPU scholarship. This work was supported in part by the Swedish Strategic Research Foundation (SSF) for the integrated program “Biomimetic Materials Science” and by the European Commission for the NANOIMPRINT project (NMP4-CT-2005-516981) to L.Y. S.A.S. acknowledges the financial support provided by National Institutes of Health (Grant GM62314). We thank Swedish Research Council (VR) (S.N., Grant 40455901), Craafordska Stiftelsen and Carl Tryggers stiftelse for financial support. This work has been in part presented at the 20th Microscale Bioseparations (HPCE) Amsterdam 2006, the fourth International Workshop on Molecular Imprinting (MIP2006), Cardiff, 2006, and Nanotech, Montreux, 2006, NanoBiotech, Stockholm 2006, Swiss Chemical Society Fall Meeting Zurich 2006.

References

1. Xie C, Fu H, Hu J, Zouq H. *Electrophoresis* 2004;25:4095–4109. [PubMed: 15597414]
2. Nilsson C, Nilsson S. *Electrophoresis* 2006;76–83. [PubMed: 16315166]
3. Eeltink S, Kok WT. *Electrophoresis* 2006;27:84–96. [PubMed: 16315168]
4. Malik A. *Electrophoresis* 2002;23:3973–3992. [PubMed: 12481288]
5. Kapnissi-Christodoulou CP, Zhu X, Warner IM. *Electrophoresis* 2003;24:3917–3934. [PubMed: 14661227]

6. Yan, M.; Ramström, O., editors. *Molecularly Imprinted Materials*. Science and Technology. New York: Marcel Dekker; 2005.
7. Schweitz L, Andersson LI, Nilsson S. *Anal. Chem* 1997;69:1179–1183.
8. Spégel P, Schweitz L, Nilsson S. *Electrophoresis* 2001;22:3833–3841. [PubMed: 11699926]
9. Spégel P, Schweitz L, Nilsson S. *Anal. Chem* 2003;75:6608–6613. [PubMed: 16465715]
10. Nilsson J, Spégel P, Nilsson S. *J. Chromatogr., B* 2004;804:3–12.
11. Nilsson C, Viberg P, Spégel P, Jörnten-Karlsson M, Petersson P, Nilsson S. *Anal. Chem* 2006;78:6088–6095. [PubMed: 16944888]
12. Amini A, Paulsen-Sorman U, Westerlund D. *Chromatographia* 1999;50:497–506.
13. Valtcheva L, Mohammad J, Pettersson G, Hjerten S. *J. Chromatogr* 1993;638:263–267.
14. Svec F. *J. Sep. Sci* 2005;28:729–745. [PubMed: 15940819]
15. Jorgenson JW, Lukacs KD. *J. Chromatogr* 1981;218:209–216.
16. Spégel P, Nilsson S. *Am. Lab* 2002 July;:29–33.
17. Behnke B, Johansson J, Bayer E, Nilsson S. *Electrophoresis* 2000;21:3102–3108. [PubMed: 11001206]
18. Rampey AM, Umpleby RJ, Rushton GT, Iseman JC, Shah RN, Shimizu KD. *Anal. Chem* 2004;76:1123–1133. [PubMed: 14961747]
19. Andersson HS, Koch-Schmidt AC, Ohlson S, Mosbach K. *J. Mol. Recognit* 1996;9:675–682. [PubMed: 9174956]
20. Ye L, Weiss R, Mosbach K. *Macromolecules* 2000;33:8239–8245.
21. Perez N, Whitcombe MJ. *J. Appl. Polym. Sci* 2000;77:1851–1859.
22. Dawkins, JV. *Aqueous Suspension Polymerisation in Comprehensive Polymer Science*. Allen, G.; Bevington, JC., editors. Oxford, UK: Pergamon Press; 1989.
23. Ugelstad J, El-Aasser MS, Vanderhoff JW. *Polym. Lett. Ed* 1973;11:503.
24. Vaihinger D, Landfester K, Kräuter I, Brunner H, Tovar GEM. *Macromol. Chem. Phys* 2002;203:1965–1973.
25. Asua JM. *Prog. Polym. Sci* 2002;27:1283–1346.
26. Edward SH, Shamsi SA. *J. Chromatogr., A* 2000;903:227–236. [PubMed: 11153946]
27. Shamsi SA, Akbay C, Warner IM. *Anal. Chem* 1998;70:3078–3083.
28. Shamsi SA, Palmer CP, Warner IM. *Anal. Chem* 2001;73:140A–149A.
29. Palmer CP, McCarney JP. *J. Chromatogr., A* 2004;1044:159–176. [PubMed: 15354436]
30. Shamsi SA, Iqbal R, Akbay C. *Electrophoresis* 2005;26:4138–4152. [PubMed: 16252318]
31. Khaledi MG, Trone MD. *Anal. Chem* 1999;71:1270–1277. [PubMed: 10204032]
32. Khaledi MG, Trone MD. *Electrophoresis* 2000;21:2390–2396. [PubMed: 10939450]
33. Macossay J, Shamsi SA, Warner IM. *Tetrahedron Lett* 1999;40:577–584.
34. Turiel E, Martin-Esteban A. *J. Sep. Sci* 2005;28:719–728. [PubMed: 15938181]
35. Ye L, Surugiu I, Haupt K. *Anal. Chem* 2002;74:959–964. [PubMed: 11924998]
36. Sellergren, B., editor. *Molecularly Imprinted Polymers: Man-made Mimics of Antibodies and their Applications in Analytical Chemistry*. New York: Elsevier; 2001.
37. Cormack PAG, Elorza AZ. *J. Chromatogr., B* 2004;804:173–182.
38. Iqbal R, Rizvi SAA, Shamsi SA. *Electrophoresis* 2005;26:4127–4137. [PubMed: 16211542]
39. Xue Q, Yeung ES. *Nature* 1995;373:681–683. [PubMed: 7854448]
40. Ishii Y, Yanagida T. *Single Mol* 2000;1:5–16.
41. Brasselet S, Moerner WE. *Single Mol* 2000;1:17–23.
42. Schäfer B, Gemeinhardt H, Uhl V, Greulich KO. *Single Mol* 2000;1:33–40.
43. Zimmerman SC, Wendland MS, Rakow NA, Zharov I, Suslick KS. *Nature* 2002;418:399–403. [PubMed: 12140553]

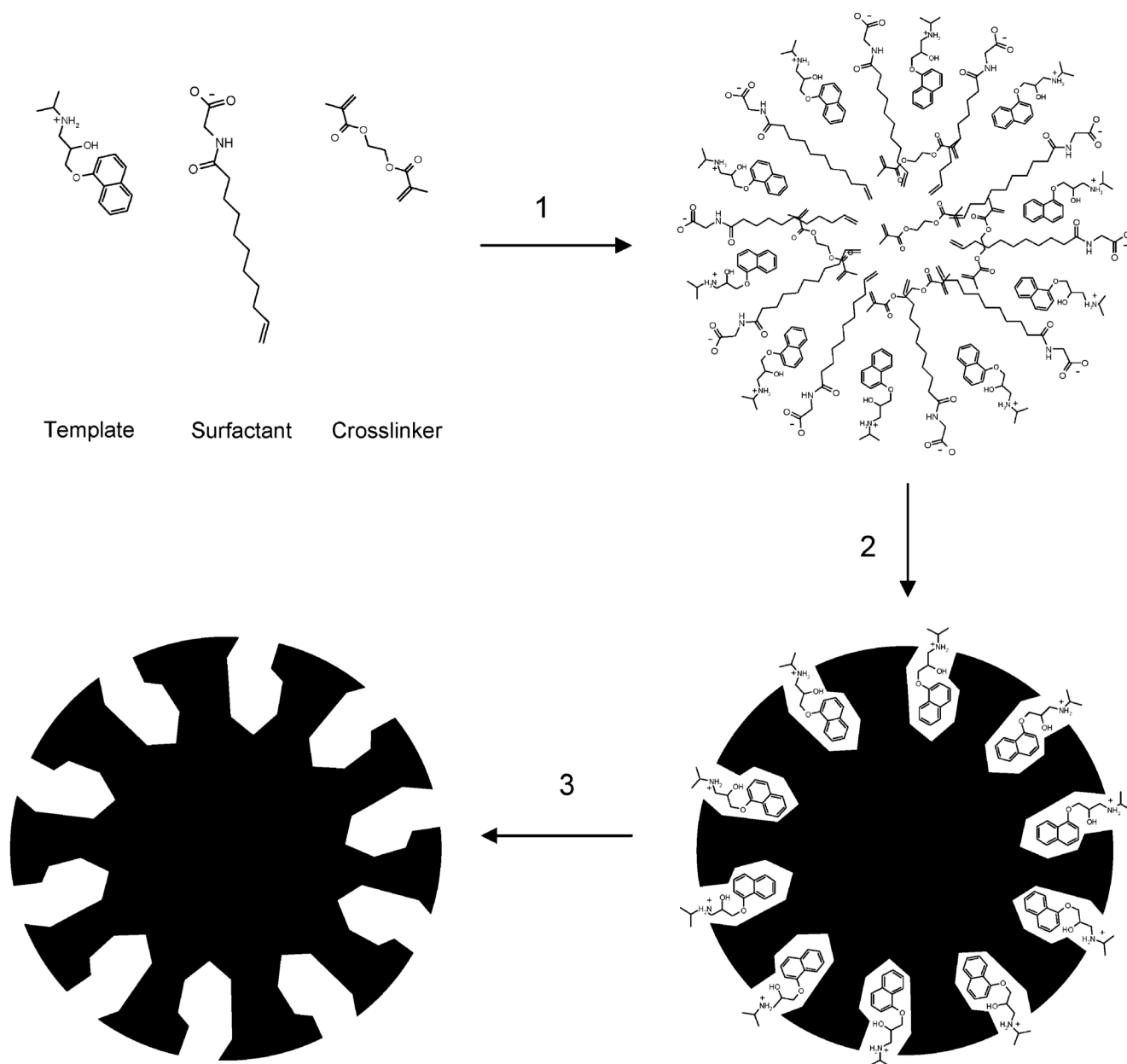


Figure 1. Synthesis of imprinted nanoparticles by miniemulsion polymerization using a functional SUG surfactant: (1) preassembly of the imprinting complex; (2) cross-linking polymerization; (3) template removal.

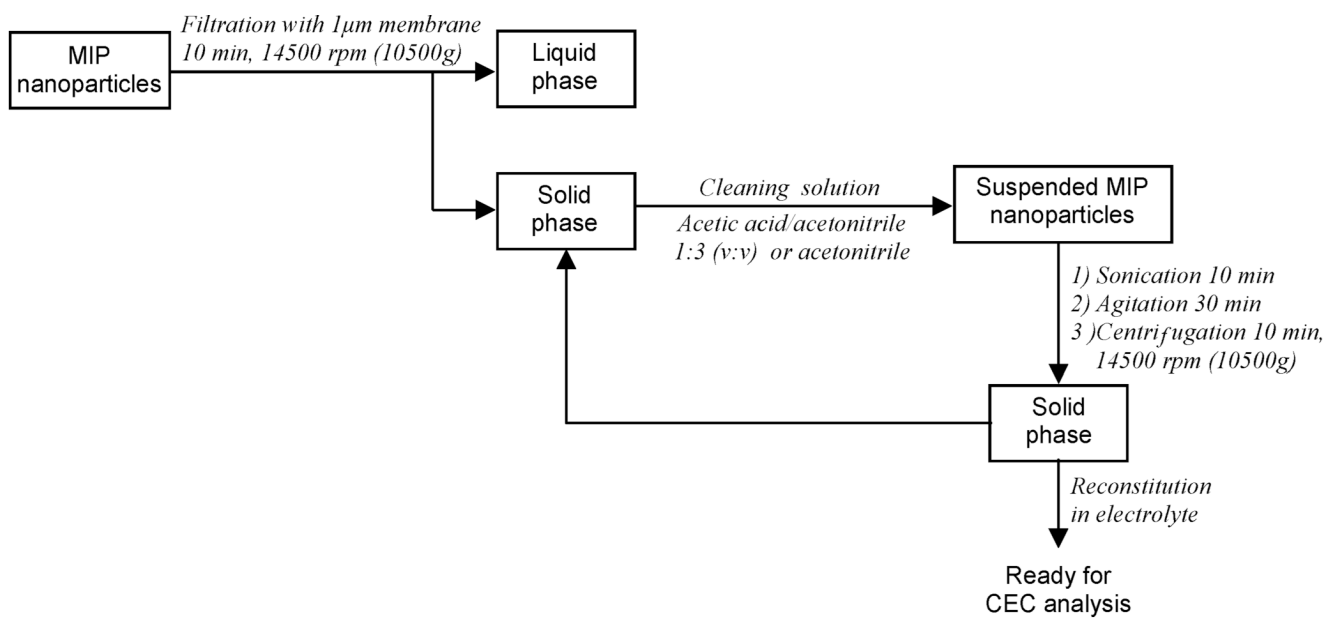


Figure 2.
Scheme for the sorting and purification of the imprinted nanoparticles.

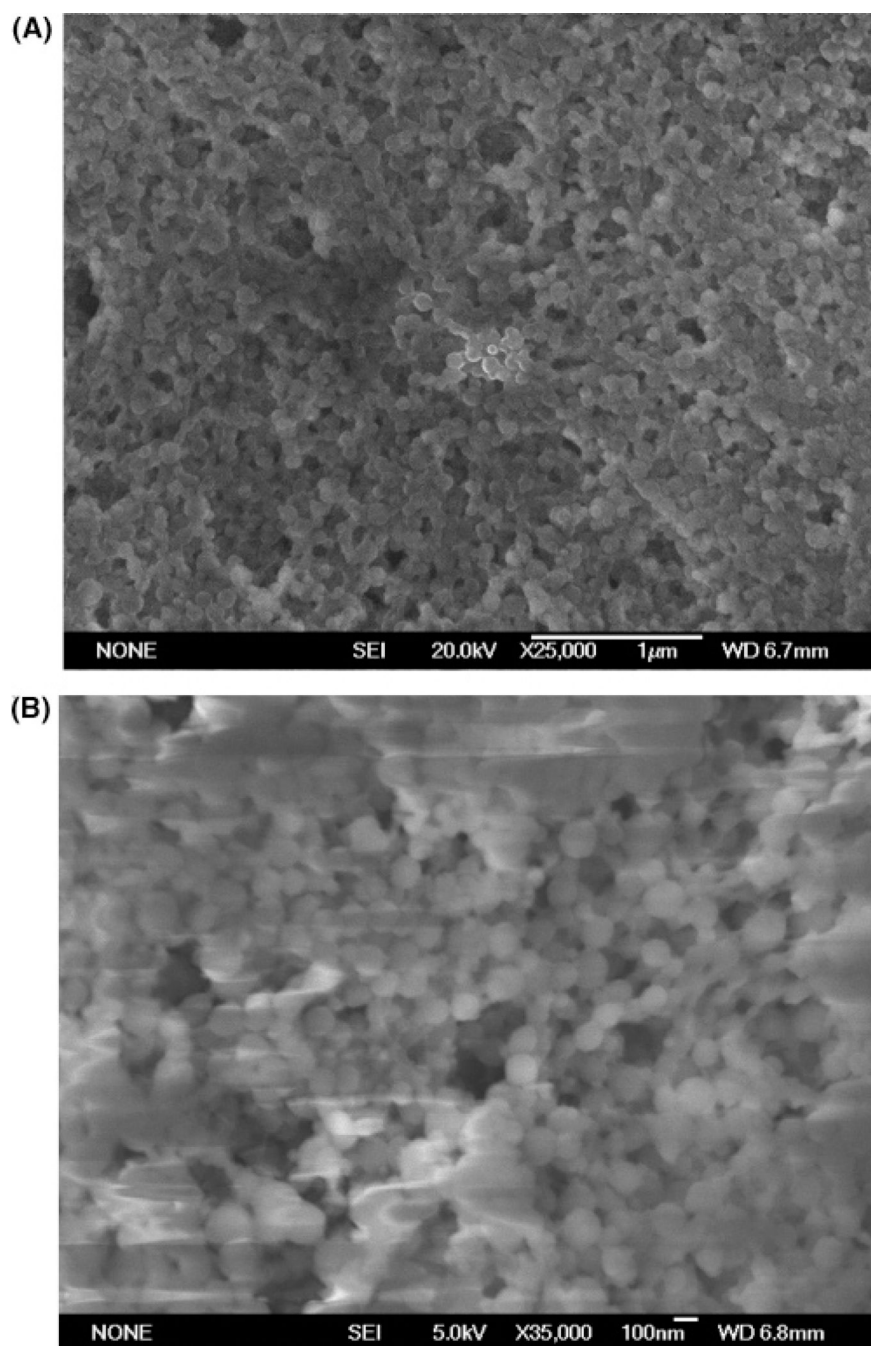


Figure 3. Scanning electron micrographs of polymeric nanoparticles prepared according to the procedure described in Experimental Section. (A) Nonimprinted nanoparticles. (B) Imprinted nanoparticles prepared with a template to functional monomer ratio of 1:11.

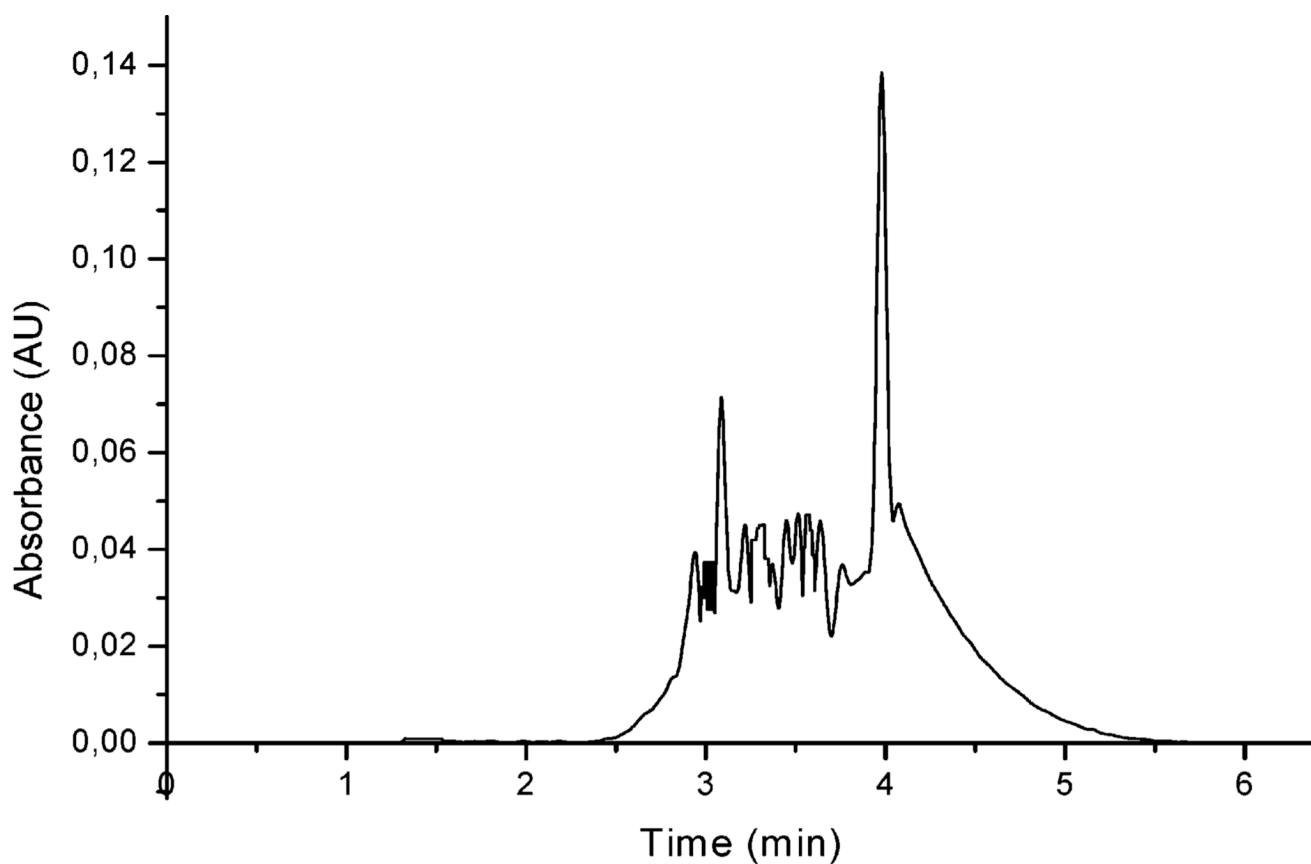


Figure 4. Electropherogram of nanoparticles (5 mg/mL) injected hydrodynamically at 0.5 psi for 5 s. Electrolyte 10 mM phosphate/20% (v/v) acetonitrile at pH 7, voltage of separation 16 kV, and temperature of the capillary 30 °C.

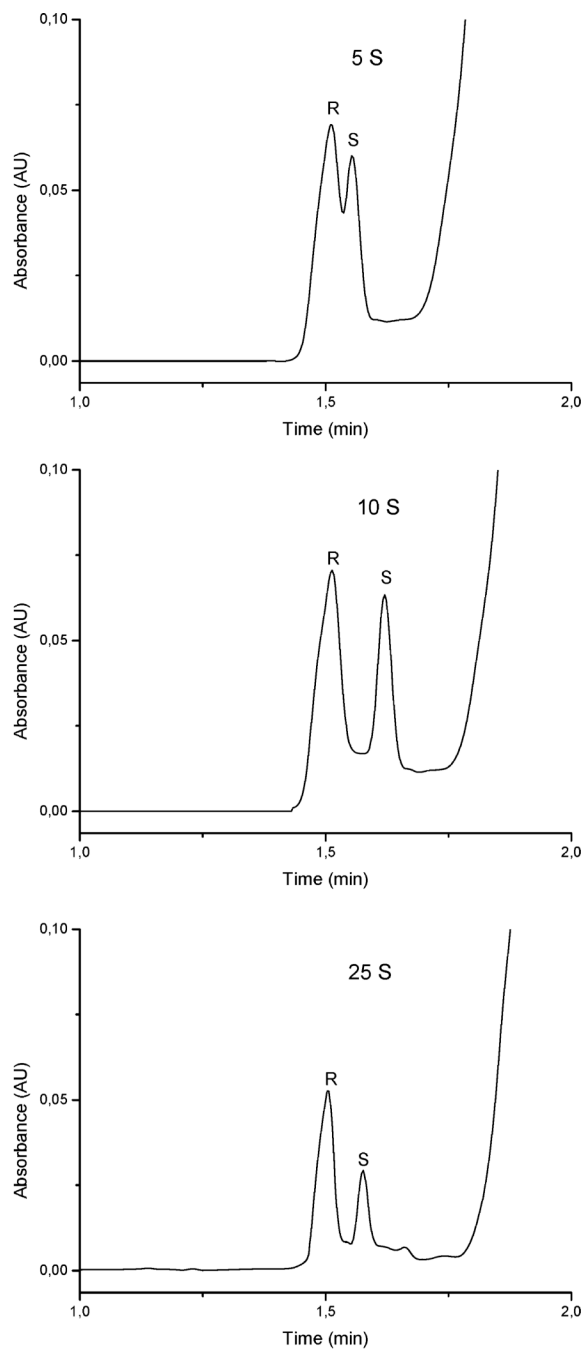


Figure 5. Optimization of the hydrodynamic injection time for nanoparticles (10 mg/mL) at 0.5 psi (5, 10, and 25 s). Injection of *rac*-propranolol (150 μ M) for 3 s at 6 kV, electrolyte 10 mM phosphate/20% (v/v) acetonitrile at pH 7, voltage of separation 16 kV, and temperature of the capillary 25 $^{\circ}$ C.

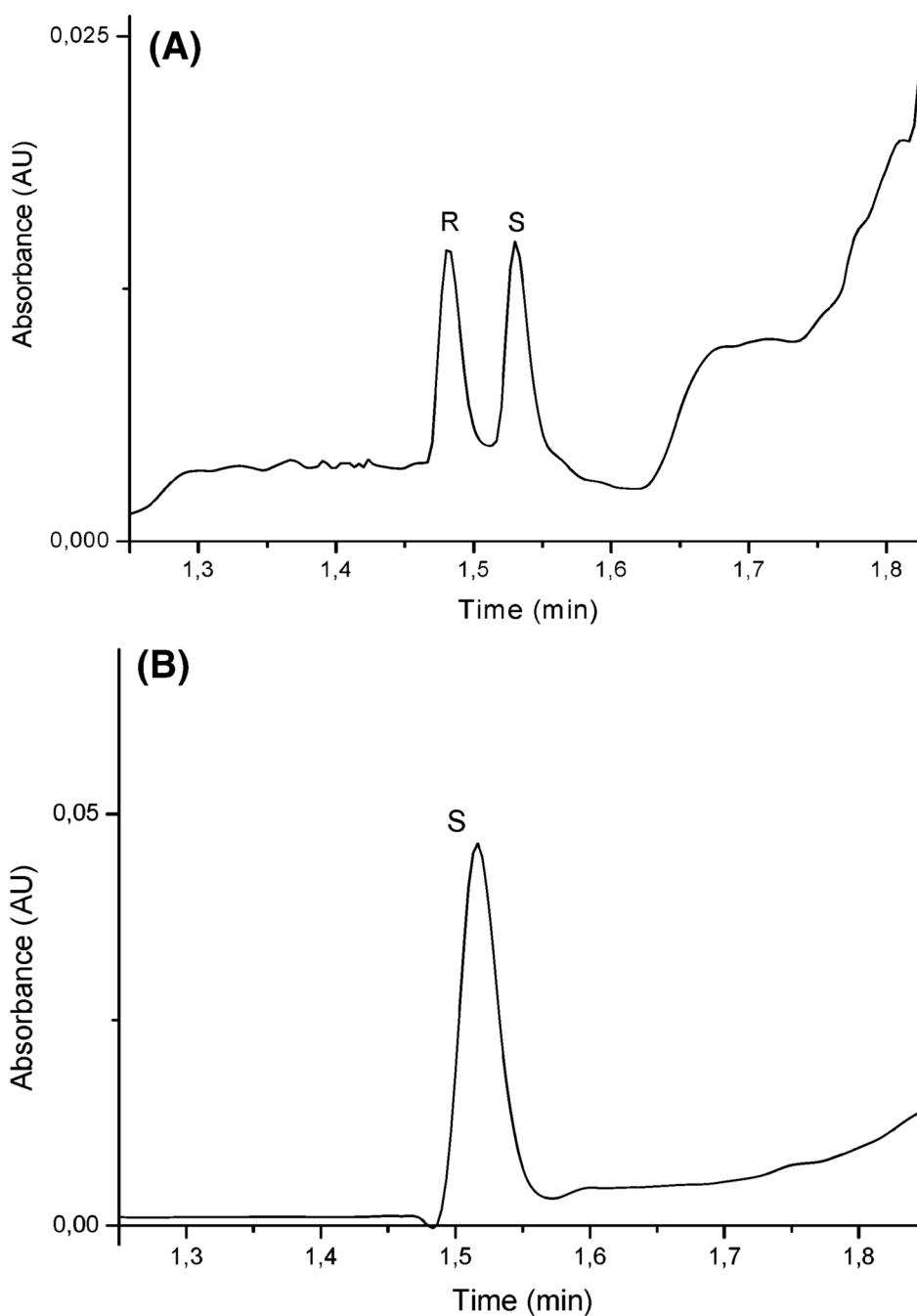


Figure 6. CEC analysis of (A) *rac*-propranolol and (B) (*S*)-propranolol (60 μ M) demonstrating the imprinting effect and identifying the peaks. Nanoparticle hydrodynamic injection (10 mg/mL) 0.5 psi for 10 s, sample injection 3 s at 6 kV, electrolyte 10 mM phosphate/20% (v/v) acetonitrile at pH 7, voltage of separation 16 kV, and temperature of the capillary 30 $^{\circ}$ C.

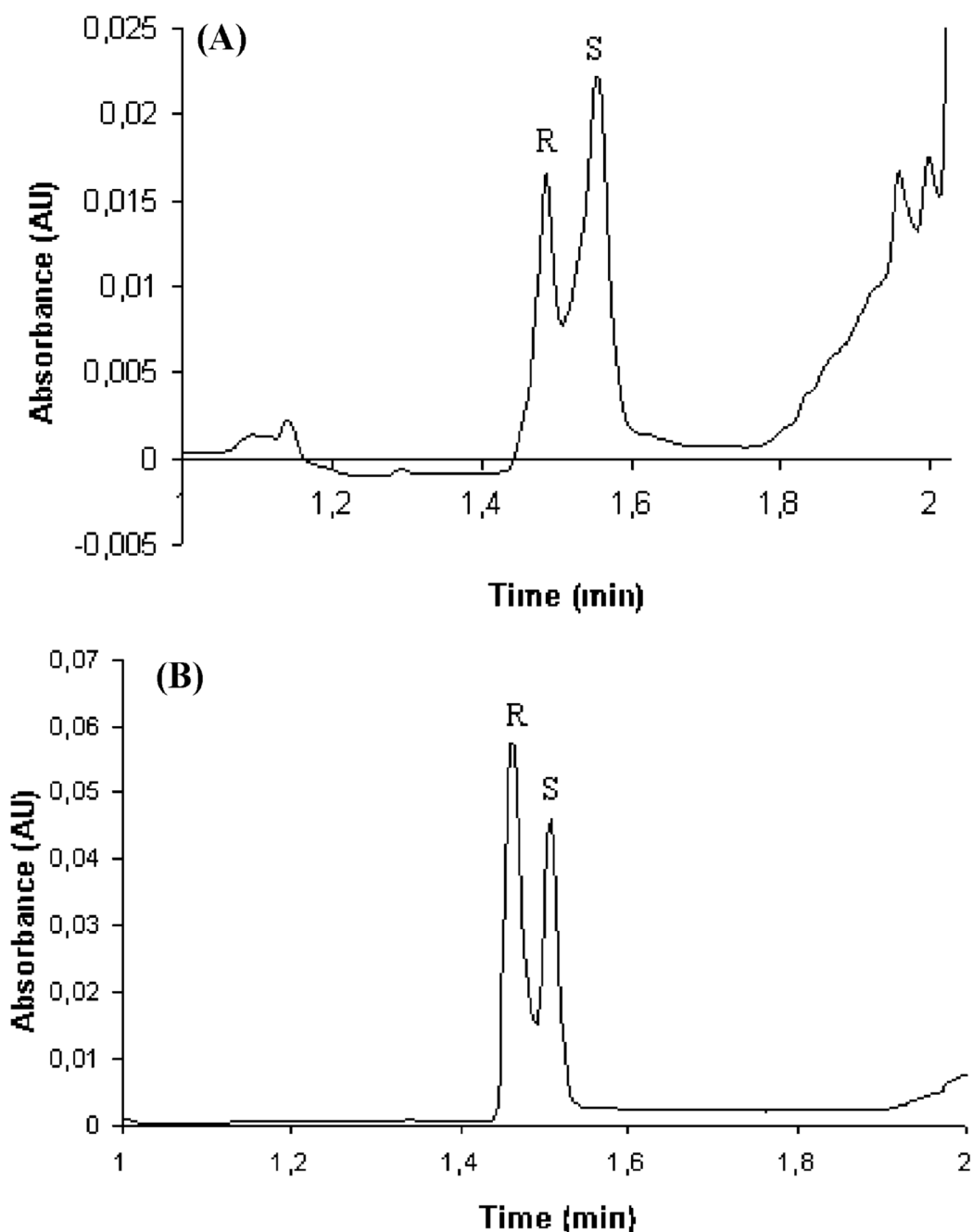


Figure 7.

Additional electropherograms confirming the enantio-separation by overloading with one of the enantiomers at time, which demonstrates the imprinting effect and enables us to identify the peaks. (A) *rac*-Propranolol (60 μ M) spiked (50% (v/v)) with (*S*)-propranolol (60 μ M). (B) *rac*-Propranolol (100 μ M) spiked (50% (v/v)) with (*R*)-propranolol (60 μ M). MIP injected hydrodynamically at 0.5 psi for 10 s, sample injection 3 s at 6 kV, electrolyte 10 mM phosphate/20% (v/v) acetonitrile at pH 7, voltage of separation 16 kV, and temperature of the capillary 30 $^{\circ}$ C.